Depth to Bedrock Estimations Using the H/V Spectral Ratio in the San Joaquin Valley

A Senior Project
Presented to

The Faculty of the Natural Resources Management and Environmental Sciences Department
California Polytechnic State University, San Luis Obispo

In Partial Fulfillment
of the Requirements for the Degree
Bachelor of Science in Earth Sciences

by

Tyler A. Morelli

August, 2013

© 2013 Tyler A. Morelli

Senior Project Adviser:
Dr. John J. Jasbinsek
Physics Department

Department Head:
Dr. Doug Piirto
Natural Resources Management and Environmental Sciences

Submitted in full collaboration with advising author:

Dr. John J. Jasbinsek
Physics Department, California Polytechnic State University, San Luis Obispo, CA 93407, USA

ABSTRACT

Basin depth is a fundamental parameter in many types of geologic studies such as resource exploration and regional tectonic mapping. The Horizontal-to-Vertical Spectral Ratio ("H/V") method has been successfully applied to estimating of basin depths up to several hundred meters. In this study the H/V method is applied to the deep basins on the western side of the San Joaquin Valley to determine the thickness of the sedimentary layers and depth to bedrock. Microtremor data from Earthscope Seismic Array stations are ideal to test the accuracy of the H/V method on deeper basins because the data is of high-quality and the proximity of several station locations to where independent basin depth estimates exist. The H/V method is also attractive because it is inexpensive and non-invasive, thus providing a reconnaissance tool for identifying locations in which more detailed mapping techniques may be justified. This study finds that while moderate basin depths (< ~1.2 km) are estimated accurately, deep basin depths (up to ~4 km) are significantly underestimated (~ 29%). These mixed results suggest that the sedimentary to bedrock transition in the deeper parts of the San Joaquin Valley is gradual rather than sharp.

TABLE OF CONTENTS

Abstract……...……iii

List of Figures….....v

Introduction…….……..…..1

Data and Methods……3

Results……..6

Site T05C…….6

Sites S05C, Q04C, R04C, and T06C……...8

Discussion……8

Conclusions……11

References Cited……25

Appendix……28

LIST OF FIGURES

1. IRIS web based time-series builder….……12
2. Locations of seismic stations……...12
3. Unfiltered microtremor data (T05C)……13
4. Smoothed microtremor data (T05C)……13
5. Frequency spectrum (T05C)……14
6. Transfer function (T05C)…….14
7. One open-end pipe harmonics…….15
8. Site response and transfer function……..15
9. Simple two layer model……...16
10. Location map (Central Valley)……17
11. Structural model (Central Valley)……18
12. Sonic log curve fitting plot……..18
13. Transfer function (S05C)…….19
14. Transfer function (Q04C)……19
15. Transfer function (R04C)…….20
16. Transfer function (T06C)…….20
17. Depth-frequency relationship……...21
18. Three-dimension plot (vary f_r, v_s)……..21
19. Three-dimension plot (vary f_r, x)……...…...22
20. Three-dimension plot (vary v_s, x) 0.01 Hz …….22
21. Three-dimension plot (vary v_s, x) 0.1 Hz ……...23
22. Three-dimension plot (vary v_s, x) 0.01 Hz …….23
23. H/V – S/R method comparison……24

INTRODUCTION

Accurate knowledge of basin depths is an important parameter to many geologic studies. This is especially pertinent for the quaternary geologist/geomorphologist interested in depositional history (Ingersoll, 1988). Geologic studies that take place on sediment filled basins require the determination of depths to bedrock, the relation between depositional environments and tectonics, and geologic parameters about the sub-soil. Precise knowledge of soft sediment cover above the bedrock is crucial for preparing cross sections and understanding the relative locations of lithologic layers. Subsurface geology can also be applied to resource extraction (gas/oil/geothermal) or groundwater studies that require information to develop efficient drilling plans or add more continuous spatial information (Lane *et al.*, 2008).

Vibroseis is a seismic method commonly used in exploration seismology to obtain subsurface layer structure, including depth to bedrock. This method uses trucks that input vibrational energy directly into the ground to be reflected from subsurface layers and detected along a linear profile of seismometers. Another technique to determine basin depths is well drilling, where examination of core samples is used to determine depth to bedrock. Both methods provide high-quality data, but suffer from being expensive, environmentally invasive, and in the case of well data spatially sparse.

The H/V Spectral Ratio (hereafter "H/V") method provides an alternative for basin depth estimation. This technique utilizes microtremors, or ambient vibration of the earth, as signal. The term microtremors refers to small ground motions propagating through the Earth's surface not due to seismic events (earthquakes) or explosions (Seht and Wohlenberg , 1999). It has been shown in previous studies that sources of microtremors can originate from sea waves, human microtremors/activity, wind, and rainfall (Seht and Wohlenberg, 1999). These sources will

produce different frequencies of microtremors, which will affect the frequency content of the microtremor frequency spectrum. The microtremor frequency spectrum is also influenced by the local layered subsurface structure, which can cause the amplification of seismic waves and resonance of certain microtremor frequencies (Seht and Wohlenberg, 1999).

The H/V ratio was first introduced in 1989 and is defined as the ratio of the averaged horizontal-components frequency spectrum of a single three-component seismometer and that of the vertical-component measured at that point (Lermo and Chávez-García, 1993). The frequency spectrum is computed by taking the Fourier Transform of the microtremor data from each respective channel (N-S, E-W, Z).

The H/V method was originally developed to determine what are known as 'site effects' of the soft sediment cover layer. Site effects can be described as parameters about the soft layer that changes how seismic waves amplify and propagate through the medium. Another application of the H/V method this paper focuses on is the determination of the depth of sediment filled basins through simple wave mechanics.

One particularly successful study of basin depth estimation applied the H/V method to an alluvial filled basin in the Lower Rhine Embayment (Germany) where a large number of well-log control exists (Seht and Wohlengberg 1999). The study applied the H/V method on parts of the basin that were tens of meters to 1.2 km in depth. Basin depths estimated with the H/V method compared very well to drilled basin depths.

The goal of this study is to apply the H/V method to the San Joaquin Valley of California. This basin is much deeper than previous studies (3-5km), and will test the validity of the H/V ratio in deep sediment filled basins.

DATA AND METHODS

The H/V method utilizes a single three component seismometer placed on the soft sediment cover site. The original data was acquired during 'quiet' (12-1A.M.) periods to reduce the effect of human microtremors on the recording. The recording was acquired through the IRIS web based time-series builder at seismic stations T05C, S05C, T06C, R04C, and Q04C seismometer locations of the Earthscope Transposable Array (TA) (Figs. 1 and 2). One minute of data was recorded and downloaded from each seismic station. While one-minute time-series is typical in previous studies (Seht and Wohlenberg, 1999), 5, 10 and 20 minute long signals were also tested; however no significant change in spectral content of the signal or dominant frequency was observed.

The original signal (Fig. 3) was tapered, de-trended, and smoothed with a low-pass filter to remove the higher frequency microtremors (Fig. 4). This pre-processing allows for a more stable calculation of the frequency spectrum and is typical in all seismic data processing (Yilmaz, 2001). The microtremor frequency spectrum of each channel of the three-component seismometer data was obtained by performing a discrete Fourier transform on the filtered data in Matlab©. The frequency spectrum shows the relative magnitudes of the frequencies that compose a filtered seismogram (Fig. 5). Once the frequency spectrum from each component is calculated, the transfer function is computed and the resulting dominant frequency is extracted for use in the basin depth calculation (Fig. 6).

The transfer function is calculated by taking a root mean square of the sum of the frequency spectra of the horizontal components (NS and EW) divided by the vertical component frequency spectrum (Eqn. 1). This form of the transfer function was computed by Delgado *et al.*

(2000), which is slightly different from the one introduced by Seht and Wohlenberg 1999. The H/V ratio utilizes the lowest "main peak" in the transfer function in order to calculate basin depth. The main peak was interpreted as the most dominant maxima at low frequencies. It is thought that the main peak correlates to the most dominant and lowest (fundamental) resonant frequency of the basin medium.

$$T(\omega) = \left(\frac{\left[H1(\omega)^2 + H2(\omega)^2 \right]}{2Z(\omega)^2} \right)^{1/2} \tag{1}$$

The H/V method is based on modeling a sedimentary basin as a simple two layer model with a hard rock basement that acts as a node side for the resonant wave, and the surface of the basin that behaves as an open end that can move freely as the wave propagates through the sedimentary medium. This is similar to how acoustic harmonics are modeled in a one end closed and one end opened pipe (Fig. 7). In this physics model, uneven multiples of quarter wavelengths resonate in the pipe. The same principle applies with the basin (Fig. 8). Since the transfer function averages the lowest frequency "main peak" from the frequency spectra, one quarter of a wavelength corresponds to the lowest main peak frequency in the transfer function plot (Figs. 6 and 8). The resonant frequency is equal to the velocity of the wave propagating through the basin divided by the wavelength (Eqn. 2). The depth is equal to the wavelength divided by 4 therefore we can combine these two equations (Eqns. 3 and 4).

$$f_r = \frac{v_s}{\lambda} \tag{2}$$

$$m = \frac{n\lambda}{4} \quad (n = 1, 3, 5, \ldots) \tag{3}$$

$$f_r = \frac{n \cdot v_s}{4m} \tag{4}$$

<u>Equations 2-4.</u> f_r = resonant frequency, v_s = shear wave velocity, m = depth, λ = wavelength

$$v_s(z) = v_0 \cdot (1+Z)^x \tag{5}$$

$$\begin{aligned} T_o &= \int_0^m \frac{\mathrm{dz}}{v_s(z)} = \frac{1}{v_0}\int_0^m (1+Z)^{-x}\,\mathrm{dz} \\ &= \frac{1}{v_0} \cdot \frac{(1+m)^{1-x} - 1}{(1-x)} \end{aligned} \tag{6}$$

It is important to note that the H/V method assumes a strong acoustic impedance contrast (≥2:1) between the bedrock and the overlying sediments. Acoustic impedance is calculated by multiplying the velocity of the wave in the medium by the density of the medium (Fig. 9) (Lane *et al.*, 2008). The H/V method is inaccurate in geologic settings where this assumption does not hold, such as gradational contacts, cementation, weathering, or strong heterogeneity (Lane *et al.*, 2008).

The depth calculation must also take into account the changing velocity of seismic waves with depth. The velocity-depth function is given by equation 5. $Z = z / z_o$ with $z_o = 1$ meter, v_o is the surface shear wave velocity, and depth dependence of the velocity is given by x. The fundamental resonant frequency can then be calculated as $1/4T_o$ since T_o is the travel time between the bottom basement and the top of the basin. Velocity as a function of vertical depth is defined as $v(z) = dz / dt$, and the travel time T_o can be calculated (Eqn. 6). The relationship between resonant frequency and depth can then be determined algebraically (Eqns. 7 and 8). Resonant frequency (f_r) is given in Hz, shear wave velocity (v_s) in meters per second, and

depth (m) in meters. During initial calculations, values for the surface velocity and depth dependence were borrowed from previous studies (Seht and Wohlenberg, 1999).

$$f_r = \frac{1}{4T_0} = \frac{v_0\left(1-x\right)}{4\left[\left(1+m\right)^{1-x}-1\right]} \tag{7}$$

Solving for m

$$m = \left[\frac{v_0\left(1-x\right)}{4f_r}+1\right]^{1/\left(1-x\right)} - 1 \tag{8}$$

RESULTS

Depths to bedrock that were compared to the H/V method calculations were estimated from previous active-source seismic studies of crustal velocity and layering (Holbrook and Mooney, 1987) (Figs. 10 and 11), well logs near the seismic stations, and cross sections scanned from the California Well Repository on the Cal State Bakersfield campus (Appendix A-C). These depths to bedrock were then compared to the values computed from the transfer function at each site.

Site T05C

An accurate relationship between depth and the frequency of the main peak was not able to be determined accurately in the deeper part of the basin occupied by station T05C. The transfer function contains a fundamental resonant frequency of 0.116 Hz (Fig. 6). Applying the above formula for basin depth yields a 2.1 km basin depth. The bedrock was estimated from well logs and cross sections to be between 3.9 and 4.5 km (Figs. 10 and 11) (Appendix A-C) (conservation.ca.gov, 2012). This underestimates depth to bedrock by about 2km, or 50% of the

expected depth inferred from well logs and cross sections. The velocity-depth function, its depth dependence (x =0.278), and surface shear wave velocity (v_o) of 162m/s were borrowed from Seht and Wohlenberg.

Curve fitting of seismic velocities taken from a nearby sonic well log (Appendix C) yielded improved basin depth estimates compared to the v_o and x values used in the velocity-depth function by Seht and Wohlenberg. The depth calculation (Eqn. 8) contains v_o and x, therefore it is important to get these parameters as accurate as possible for the specific site. Data points representing average seismic shear wave velocity at a given depth range were chosen off of the nearby sonic well log and plotted using Matlab©'s curve fitting feature (Fig. 12). The data points were fit to the same functional form as equation 5, using the depths as the 'z' (independent variable) values and the shear wave velocities as the 'v_s' (dependent variable) values. The sonic log data starts at about 550 meters deep, which gave no information about surface shear wave velocity and made extrapolation to surface shear wave velocity poorly constrained.

Surface shear wave velocity (v_o) was extrapolated to surface depth during the curve fitting session and depth dependence (x) was estimated from the best fit curve. The curve fitting session produced a projected v_o value of 121.2m/s and an estimated x value of 0.3594. Substituting these values of v_o, x and the resonant frequency from the transfer function for station T05C in to equation 8 yields an improved basin depth estimate of 3.0km. This result underestimates the basin depth by about 1.2km or 29% of the expected depth inferred from well logs and cross sections.

Eastern Basin: Stations S05C, Q04C, R04C, and T06C.

The eastern side of the basin, adjacent to the foothills of the Sierra Nevada mountain range has a much shallower basin than the western side where station T05C is located (Fig. 2). Basin depths are shallower and thus it may be expected that the sedimentary to bedrock contact will be sharper and more accurate basin depths will be calculated.

The transfer function of the S05C station showed a fundamental resonant frequency of 0.35 Hz (Fig. 13). This correlates to a basin depth of 465 meters. This value correlates well with depths to bedrock estimated from cross sections and boreholes in the area (Appendix A-C) (conservation.ca.gov, 2013). The transfer function of the Q04C station showed a resonant frequency spike at 0.38Hz (Fig. 14), correlating to a basin depth of 416 meters. The transfer function of the R04C station contains a resonant frequency spike at 0.48Hz (Fig. 15), which correlates to a basin depth of 302 meters. The transfer function of the T06C station showed a resonant frequency spike at 0.25Hz (Fig. 16), which correlates to a basin depth of 739 meters. These values work well with previous studies that estimate this side of the basin to be about 305 to 650 meters deep (Pujol, 1954/1958)(conservation.ca.gov, 2012/3).

DISCUSSION

Calculated depth beneath the western side of the San Joaquin Valley basin near the T05C station underestimated the expected depth of about 4.2km by about 29%. This result indicates that one of the major assumptions that must be applied to the H/V method is likely not valid in the deeper part of the San Joaquin Valley (SJV). Specifically, that there must be a strong (≥2:1) acoustic impedance between the bedrock and overlying sediments (Lane *et al*., 2008). Examples of geologic setting where this assumption might not hold are gradational contacts

resulting from weathering or cementation, and strong heterogeneity within the basin (Lane *et al*., 2008). It is possible due to the deep nature of the western side of the basin that there is compaction taking place due to the significant amount of overburden above the bedrock. Compaction in the lower half of the basin would make the assumption of strong acoustic impedance invalid.

Analysis of the basin depth formula was performed on the depth dependence equation (Eqn. 8) (Seht and Wohlenberg, 1999). Two- and three-dimensional plots were made to illustrate the relationship between depth and resonant frequency, particularly to examine how these parameters trade-off in producing basin depths.

First a 2D plot was made showing the depth-frequency relationship holding the values for depth dependence and surface shear wave velocity given by Seht and Wohlenberg constant (Fig. 17). This plot illustrates that the depth dependence equation has a drastic change in behavior around the 0.15Hz frequency value. The graph becomes extremely steep, and small variations in frequency yield drastically different depth estimates. 3D plots were also made where one of the parameters (x, v_s or f_r) was held constant, and the other two were explored over a range of values (Figs. 18-22). The 3D plots showed the similar results, that the depth approximation becomes unstable for lower frequencies. The depth dependence equation becomes more stable at higher depth dependence values and surface wave velocities.

The H/V method is a 1D wave method and does not account for 2D and 3D site effects. 2D and 3D site effects can be influenced by the geometry of the basin and local geology (Yuncha and Luzón, 2000). It is possible that the seismometers are detecting 2D and 3D site effects that the method does not account for.

Good results were obtained in the eastern side of the basin where depths range from about 302 to over 600 meters. Depth values calculated from stations on this side of the basin were compared to geologic cross sections and borehole drillings from the same region. Shallower basin depths on this side of the basin mean that there is less overburden and compaction above the bedrock. This allows for strong acoustic impedance between the bedrock and overlying sediments. These results are consistent with previous studies that have been conducted in this depth range.

An alternative method that still utilizes microtremor data is the reference site method (S/R method). The S/R method uses two seismometers, one placed on the soft sediment site and one placed on a nearby bedrock site. The S/R transfer function is calculated by dividing the averaged horizontal component spectra from the soft sediment site by the averaged horizontal component spectra of the bedrock site (Fig. 23). The S/R method still tries to determine the fundamental resonant frequency of the basin. The S/R method is assumed to show something similar to site effects, which tell about how seismic waves are amplified or attenuated in the soft sediment basin. The main disadvantage of the S/R method is that it uses two seismometers. One is placed on a soft sediment site and one on a bedrock site. The two sites located at different spatial locations and having different local geology are not influenced by the same local microtremor sources. Computing the ratio becomes difficult when you divide the two frequency spectrums. The denominator and numerator spectrum in the S/R method does not divide out the higher frequencies as effectively as the H/V method since the H/V method uses a single seismometer at the same spatial location (Seht and Wohlenberg, 1999).

The H/V method can also be used to determine site effects. The H/V method tries to determine the fundamental resonant frequency of the basin below the site. The fundamental

resonant frequency, along with the amplification of ground motion is the data required to perform seismic hazard assessments (Cara *et al.*, 2008). The H/V ratio is ideal for acquiring this data because it can acquire the data in areas of low seismicity, data acquisition is short, it requires only on seismometer, and signal processing can be done quickly (Cara *et al*., 2008).

The results of this study agree with previous work applying the H/V method to sedimentary basins less than 1.2km. Sites on the eastern side of the basin estimate the depth reasonably well. While, on the deeper part of the basin the H/V method underestimated the depth by about 29%. The H/V method can be used as a valuable tool to assist borehole data where drillings are sparse and a more detailed understanding of basin depth is desired. Proof of strong acoustic impedance between the bedrock and overlying sediments must be determined prior to conducting an H/V study.

CONCLUSIONS

In this study the H/V method was applied to the much deeper sedimentary basins of the San Joaquin Valley than previous studies have addressed. The H/V method underestimates the 4.2 km basin depth at the tested seismic site by 29%. This underestimation most likely arises from a more gradational material property contrast between the sedimentary basin and the basement rock, which violates an assumption of the H/V method. Thus the only conclusion is a lower bound for basin depth. The second test site, with a more moderate basin depth near the Sierran foothills provided an accurate estimate. In the absence of a modification to the processing of microtremor data, we conclude the H/V method should only be used for basin depths thought to be < ~1.2 km thick.

FIGURES

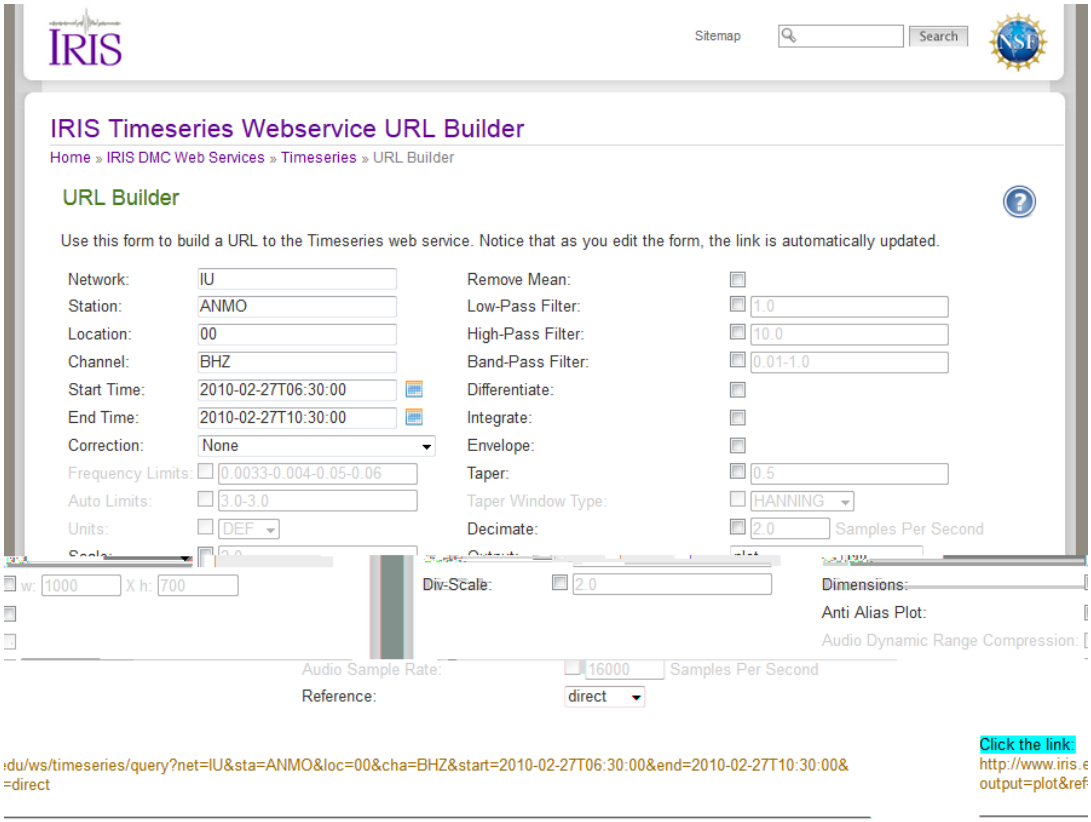

Figure 1. IRIS web based time-series builder (IRIS, 2012).

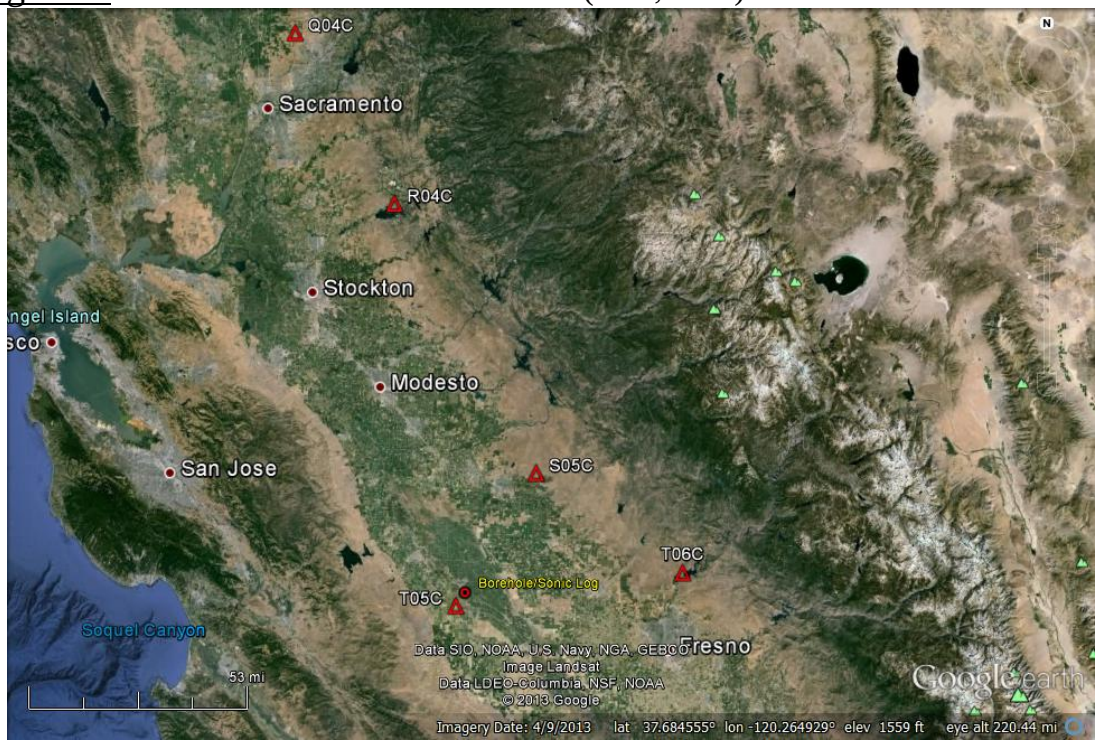

Figure 2. Locations of seismic stations. Red triangles show Easrthscope Transportable Array seismic stations in the San Jouquin Valley used in the basin depth analysis (IRIS, 2012).

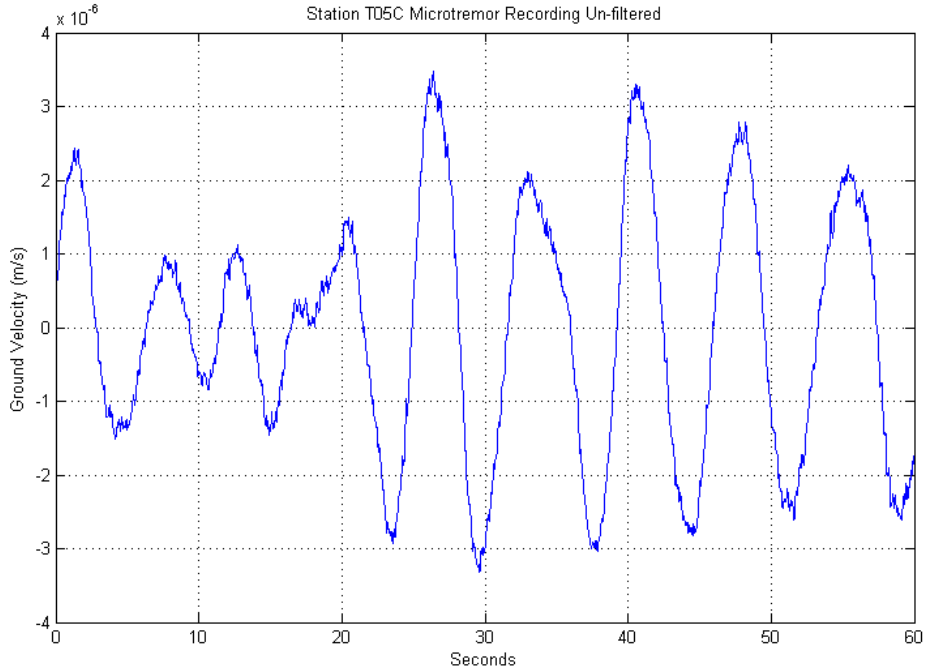

Figure 3. Unfiltered micrtotremor data. From station T05C for the vertical (Z) channel.

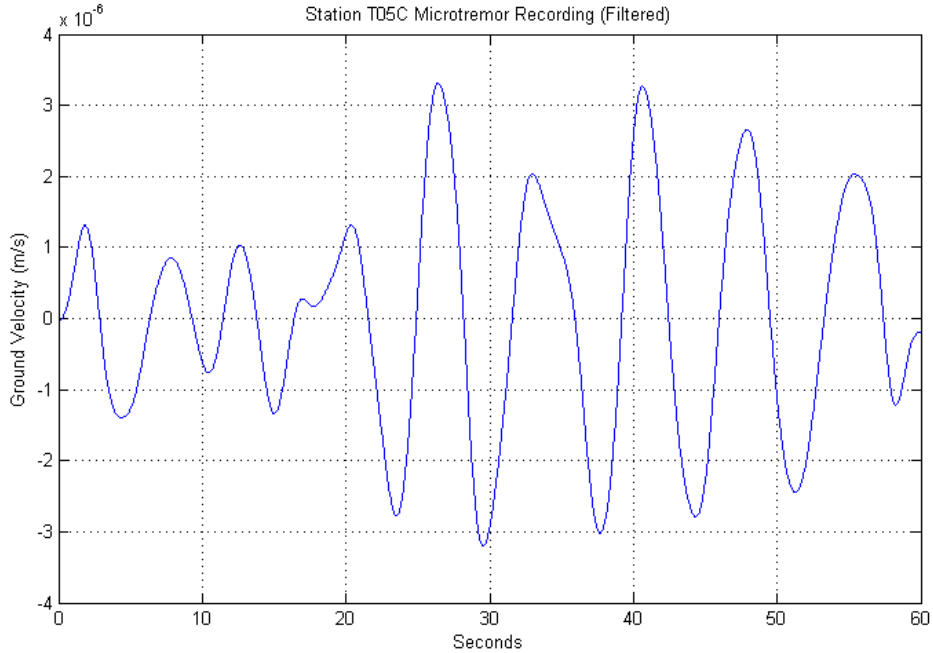

Figure 4. Smoothed microtremor data. Data from station T05C using a low-pass filter for the Z channel.

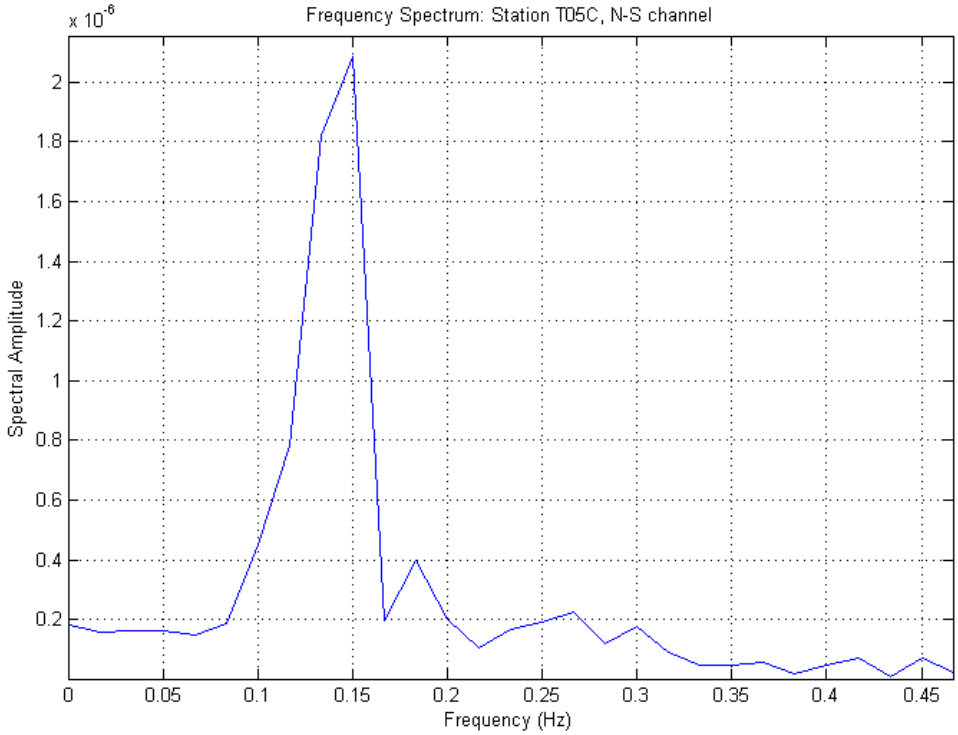

Figure 5. Frequency spectrum. N-S channel for station T05C.

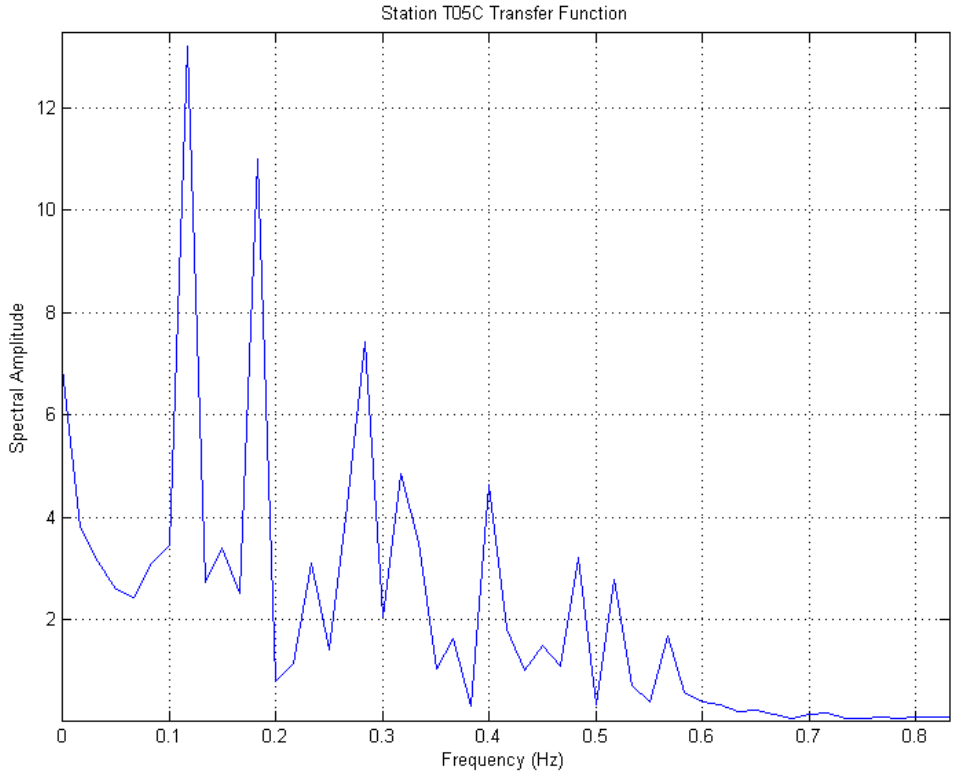

Figure 6. Transfer function. Calculated from all three channels at station T05C.

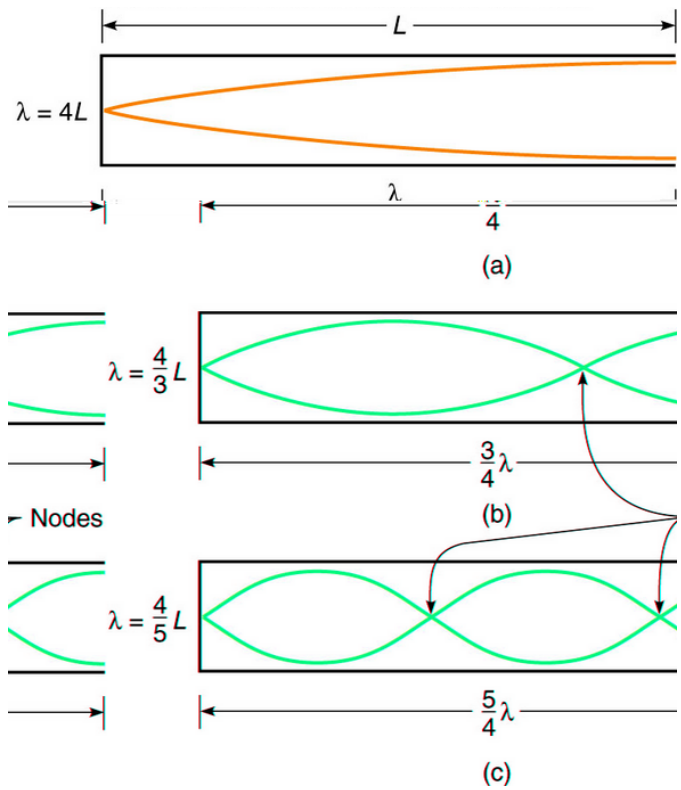

Figure 7. Harmonics in a pipe with one open end (onlinephys, 2013).

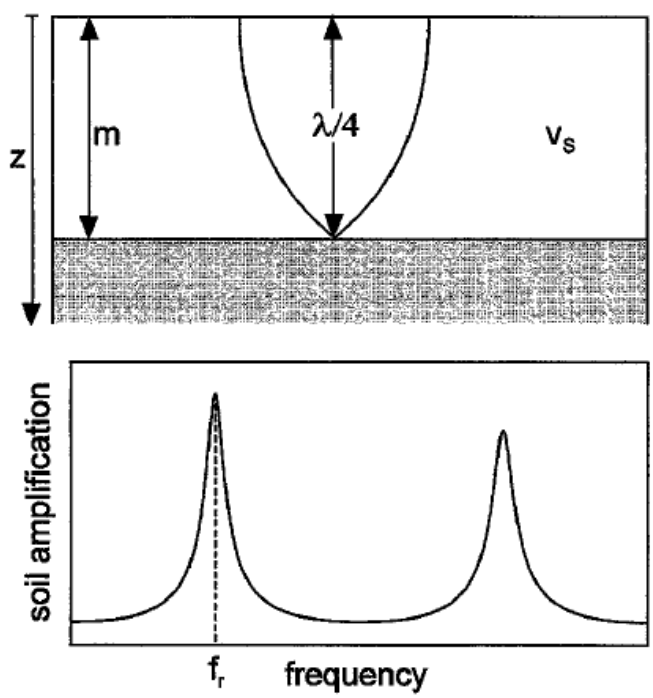

Figure 8. Site response and transfer function for a sedimentary layer over bedrock (Seht and Wohlenberg 1999).

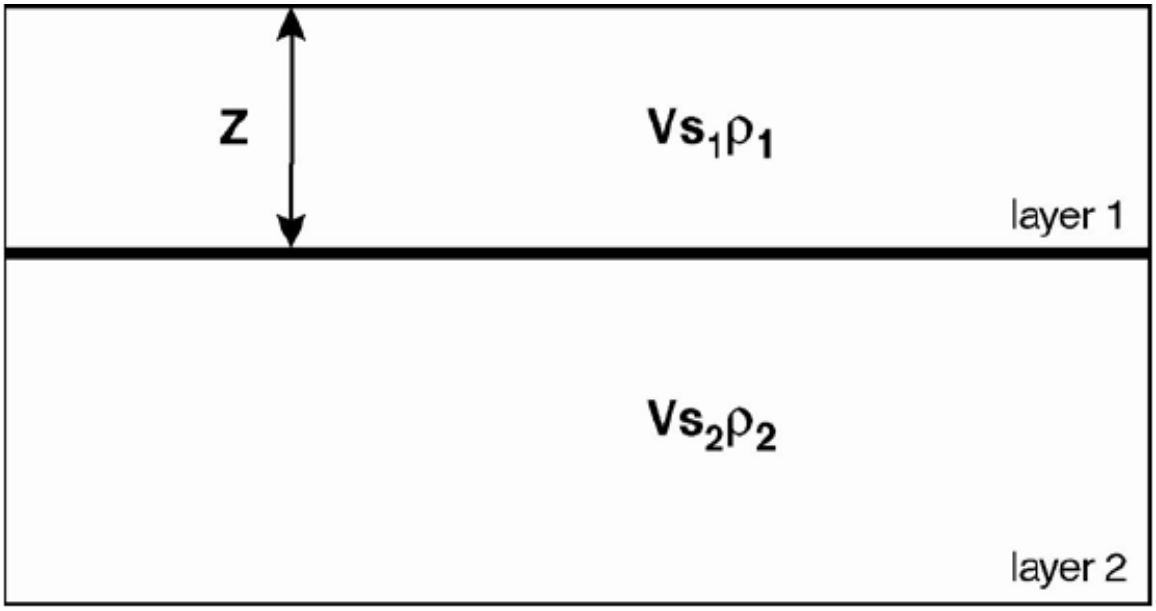

Figure 9. Simple two layer model. Defines the acoustic impedance in each layer. The H/V method assumes a strong (≥2:1) impedance contrast between the bedrock and overlying sediments (Lane *et al.*, 2008).

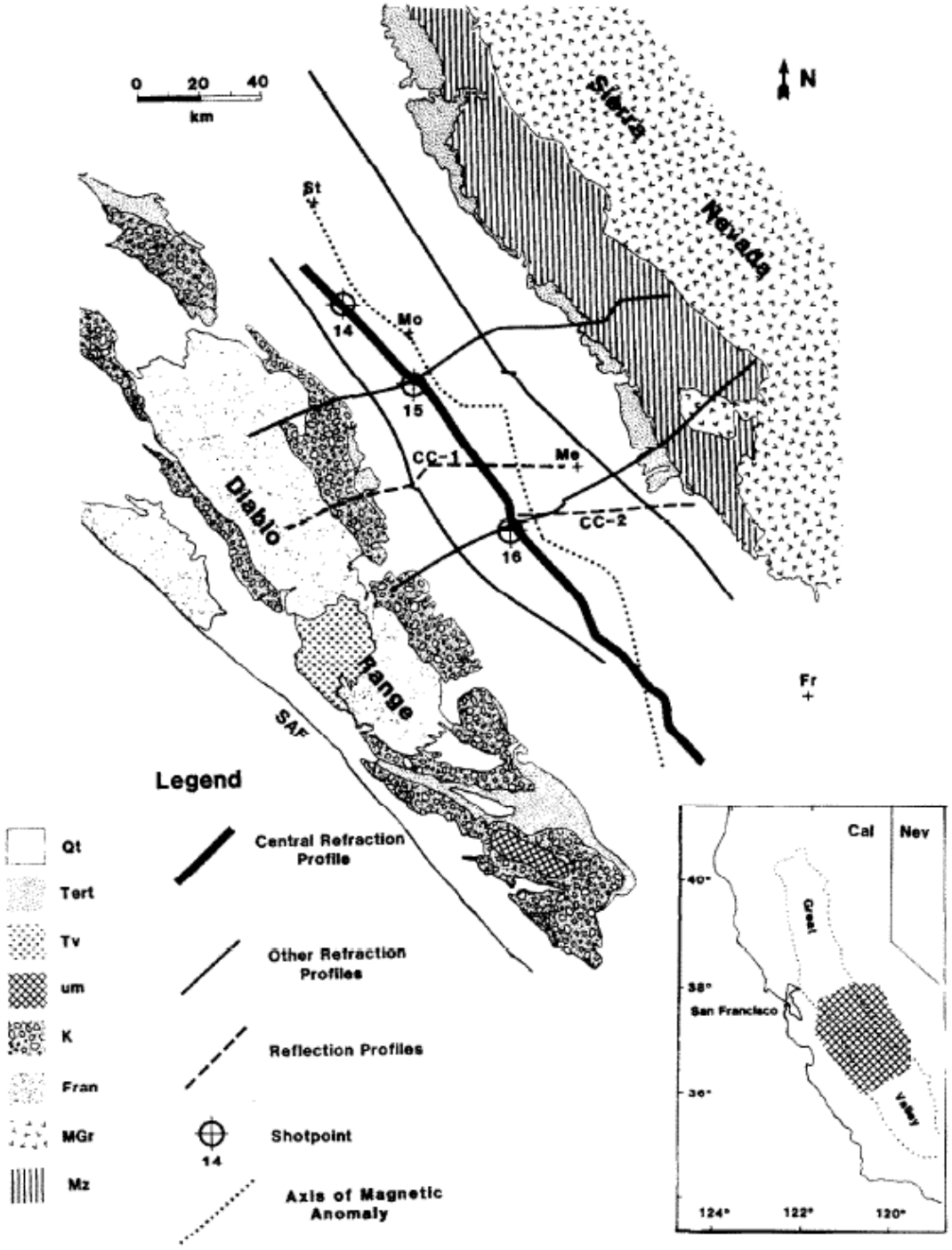

Figure 10. Location map of Central Valley, California. Showing refraction lines, reflection profiles and generalized geology (Holbrook and Mooney, 1987).

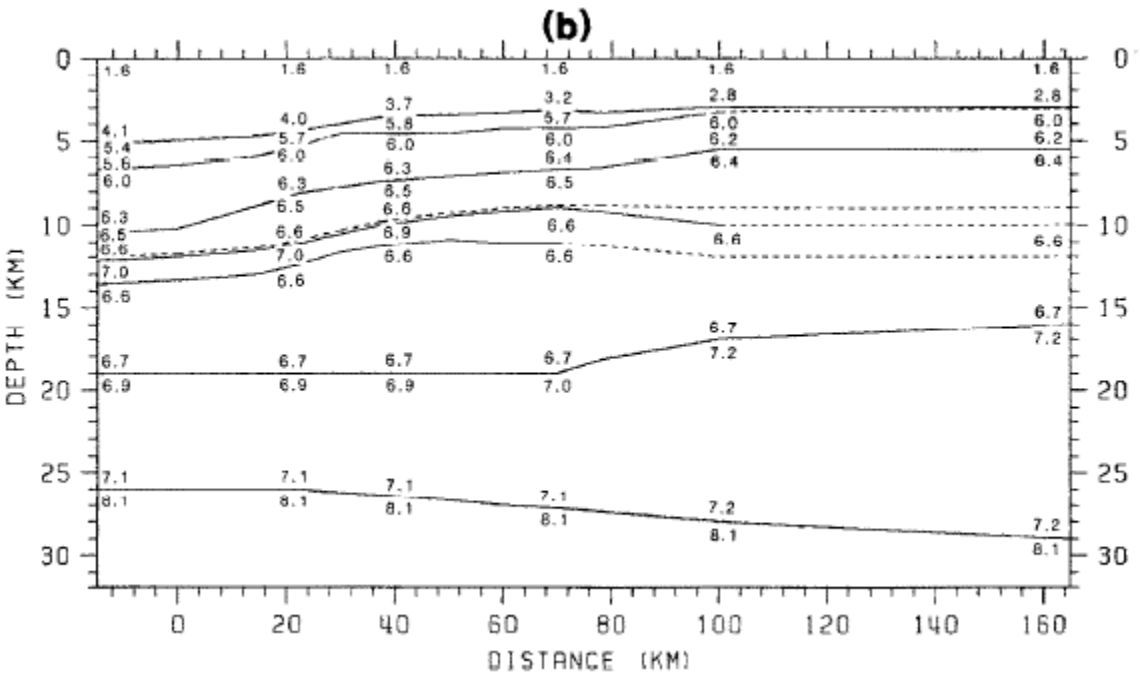

Figure 11. Structural model for central axis profile (Holbrook and Mooney, 1987).

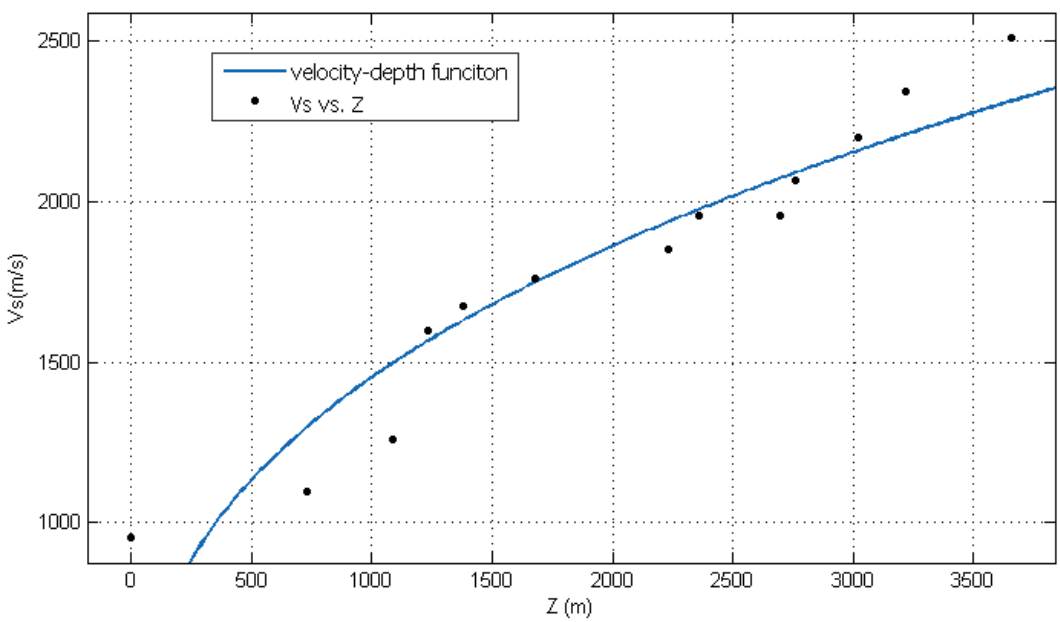

Figure 12. Sonic Log Curve Fitting Plot. Velocity-depth function in the form of equation 5 fit to data points (z , v_s) selected from nearby sonic log. Curve fitting produced a v_o value of 121.2m/s and an x value of 0.3594.

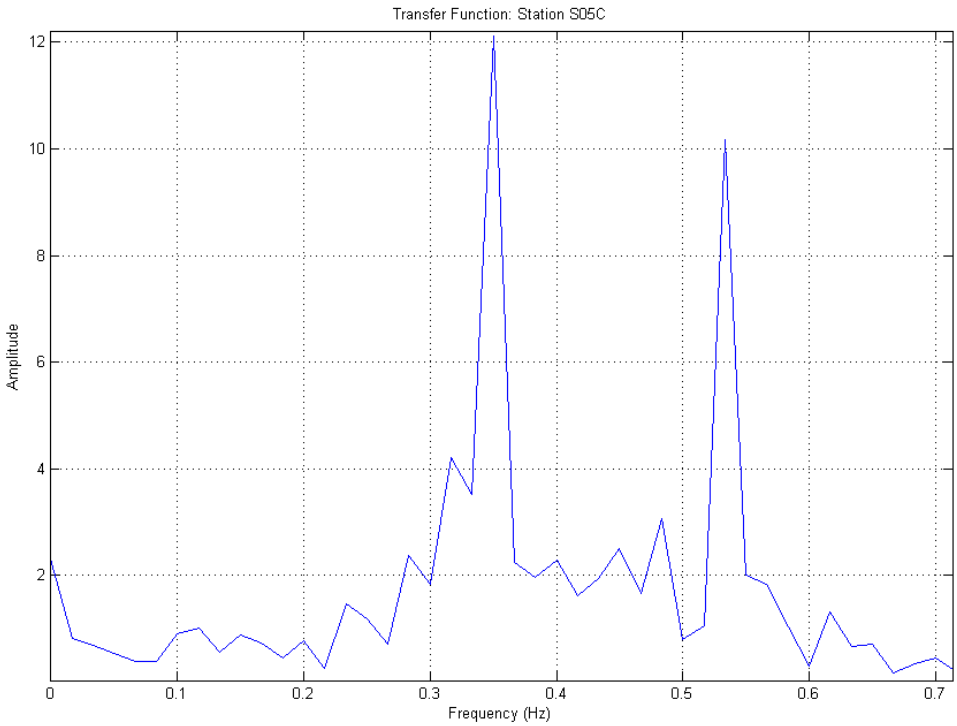

Figure 13. Transfer function. Eastern basin station S05C.

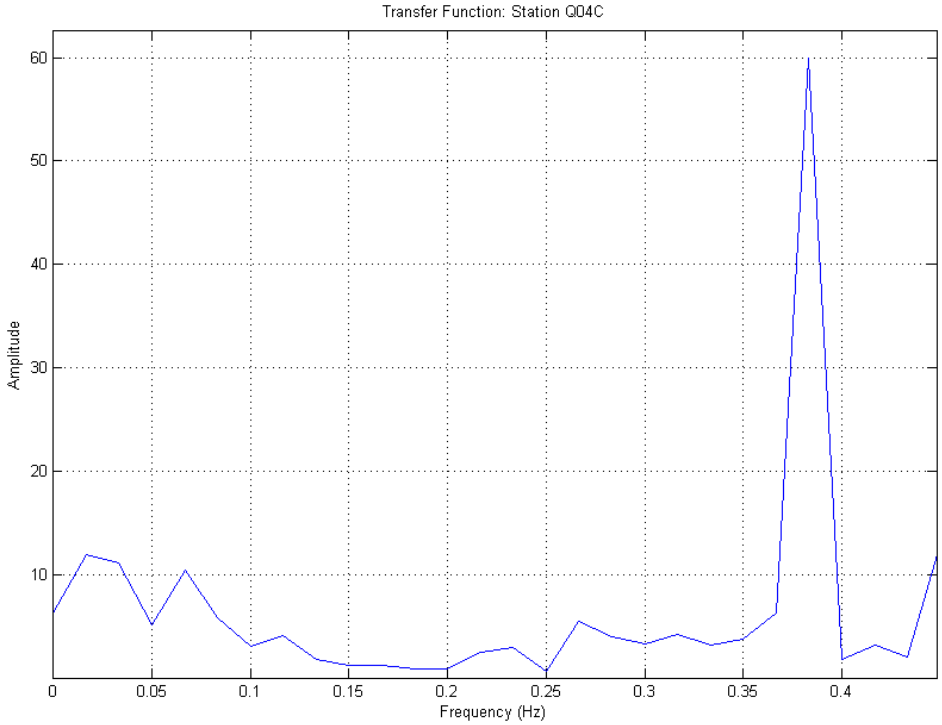

Figure 14. Transfer function. Eastern basin station Q04C.

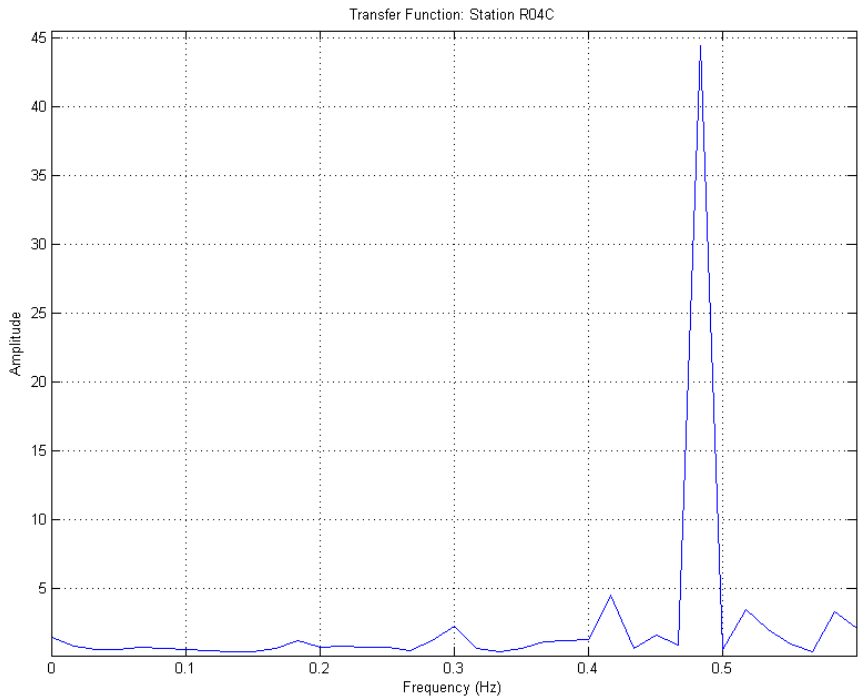

Figure 15. Transfer function. Eastern basin station R04C.

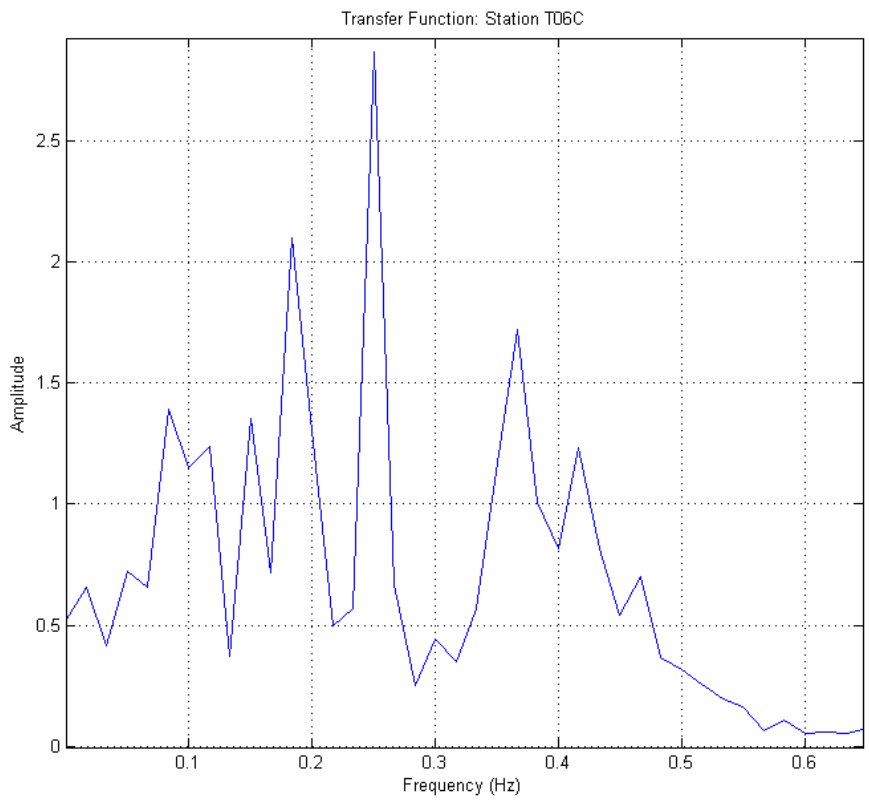

Figure 16. Transfer function. Eastern basin station T06C.

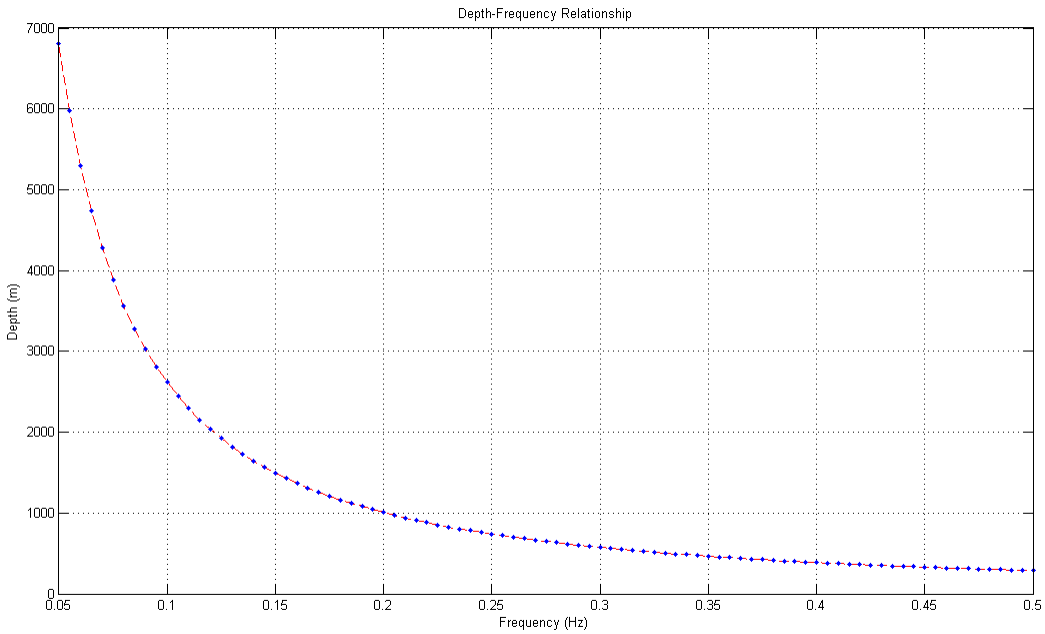

Figure 17. Two-dimension depth-frequency relationship. Plot showing depth-frequency relationship using Seht and Wohlenberg's values for surface shear wave velocity (v_s) and depth dependence (x).

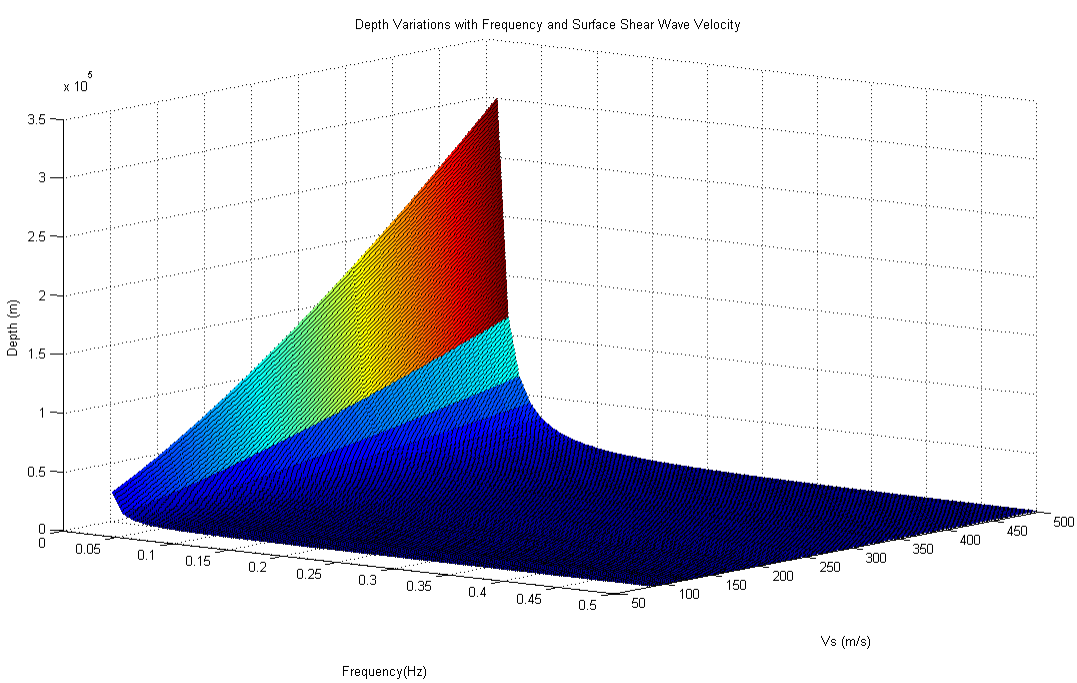

Figure 18. Three-dimension plot. Displays depth values over a range of frequencies (f_r) and v_s values using Seht and Wohlenberg's x value.

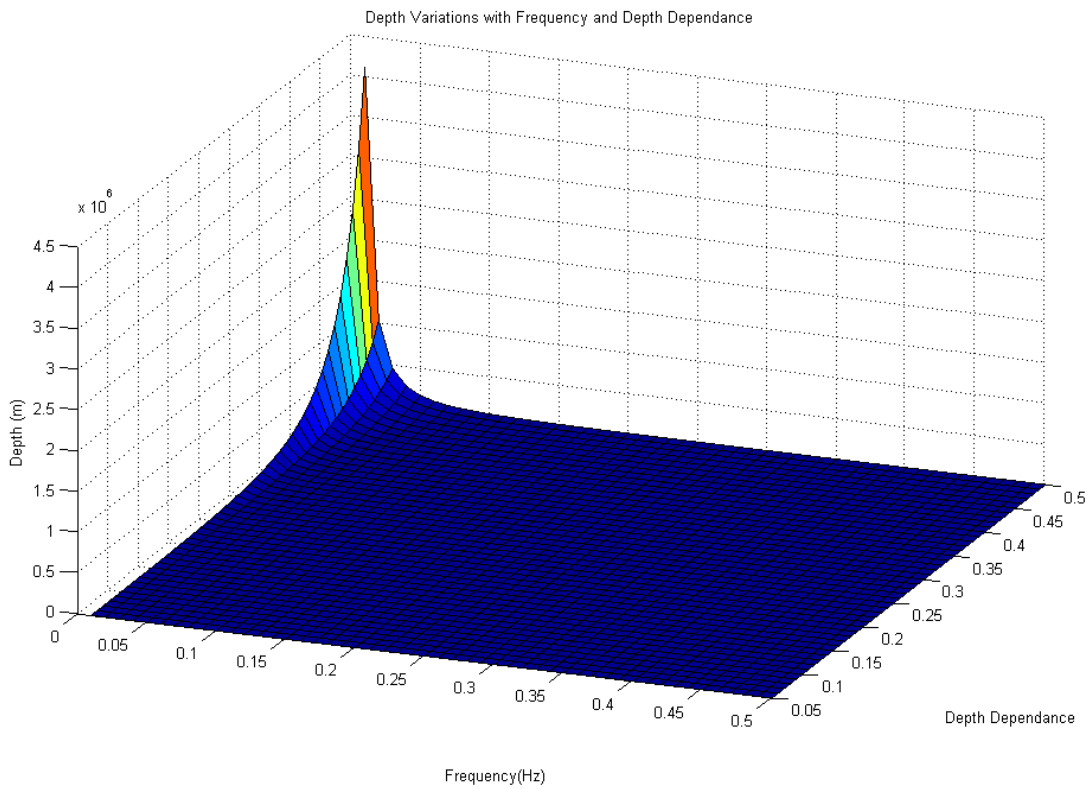

Figure 19. Three-dimension plot. Displays depth values over a range of f_r and x values using Seht and Wohlenberg's value for v_s.

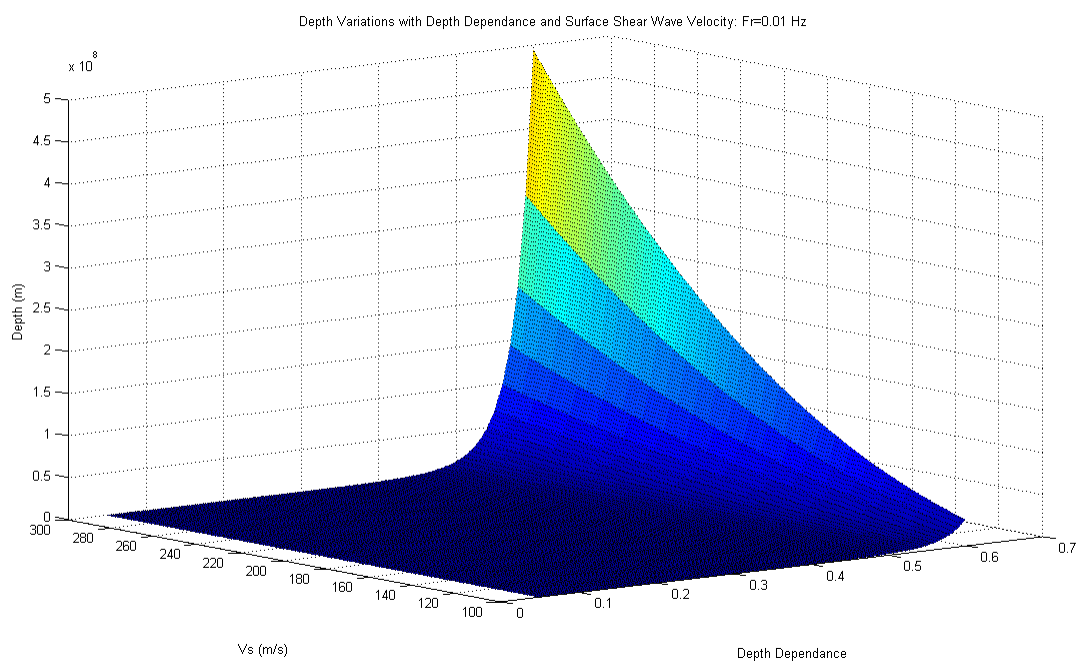

Figure 20. Three-dimension plot. Displays depth values over a range of v_s values and x values holding f_r constant at 0.01 Hz.

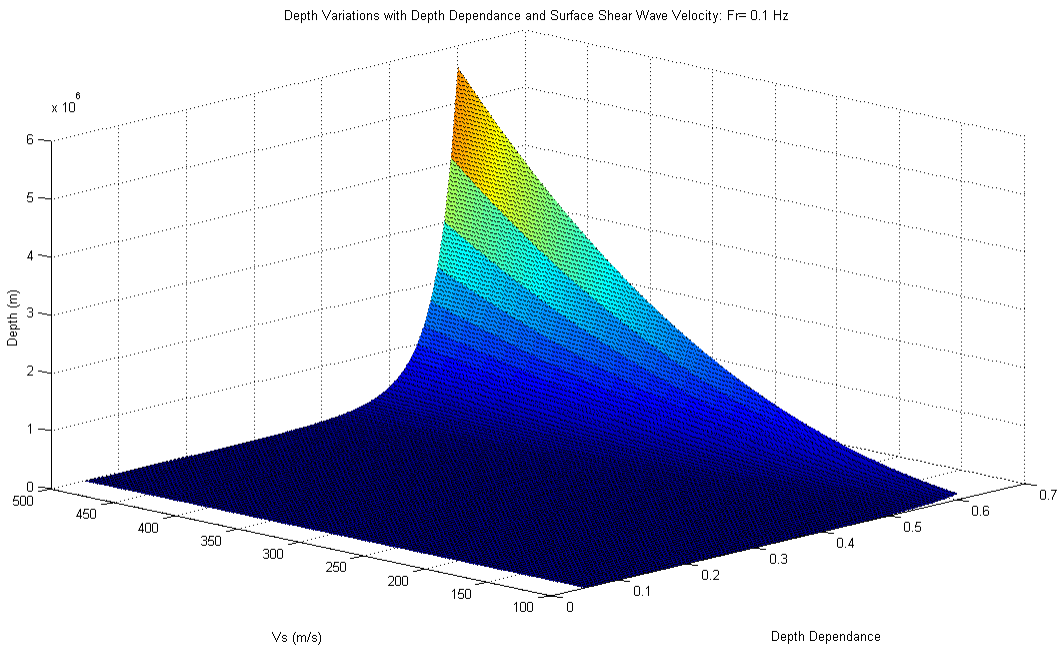

Figure 21. Three-dimension plot. Displays depth values over a range of v_s and x values holding f_r constant at 0.1 Hz .

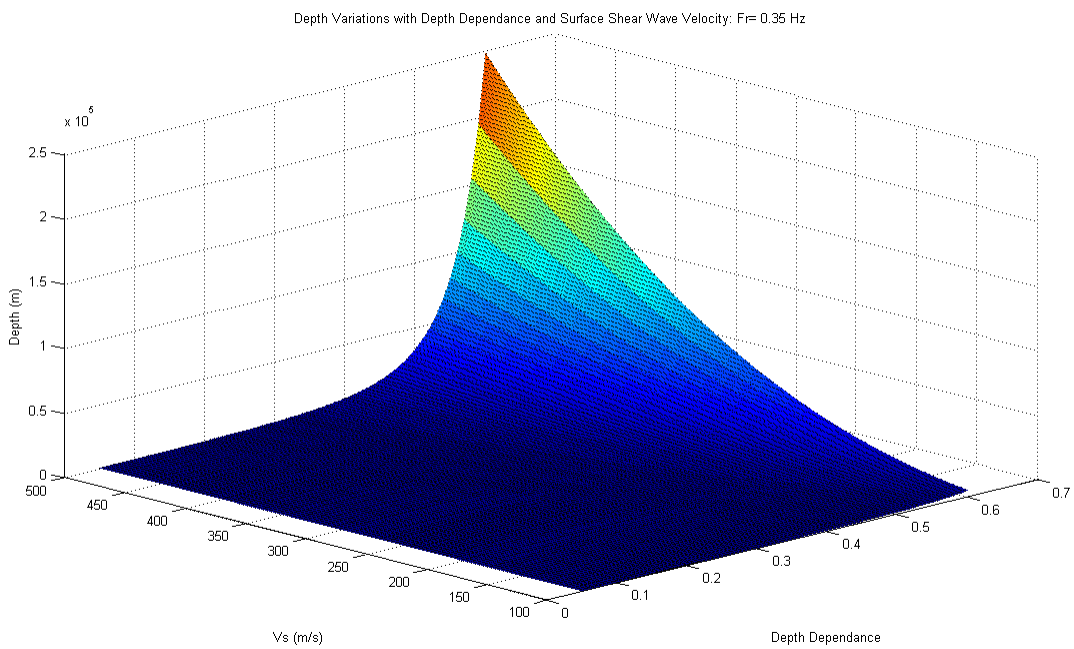

Figure 22. Three-dimension plot. Displays depth values over a range of v_s and x values holding f_r constant at 0.35 Hz .

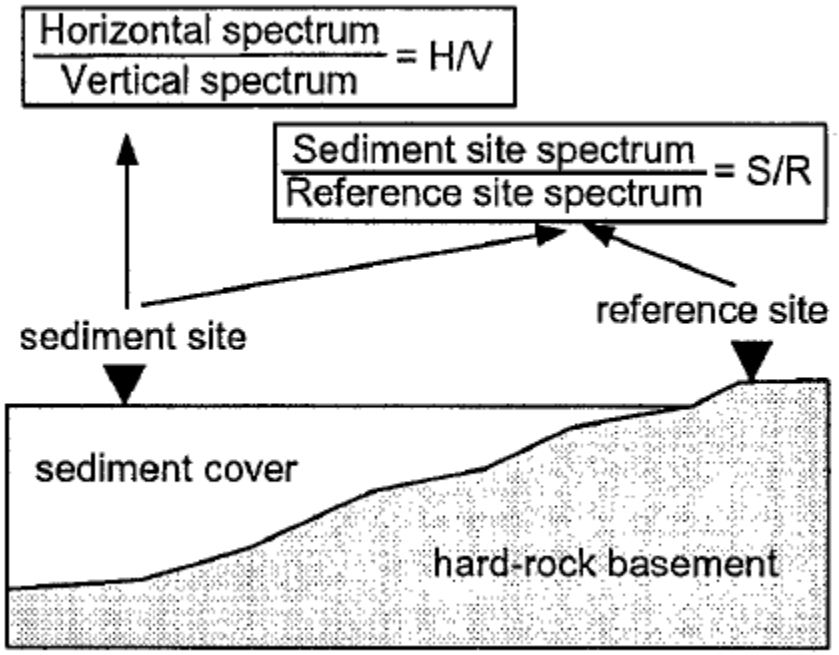

Figure 23. Various microtremor methods. Compares H/V and S/R methods that both use microtremor spectra to determine resonant frequency and/or site effects (Seht and Wohlenberg, 1999)

REFERENCES CITED

California Department of Conservation, Division of Oil, Gas, and Geothermal Resources 2012. "Sonic Log, Phillips Petroleum Company, Well: Redfern Ranches #A-1, Dos Palos Field, Section: 26, Township: 11S, Range: 12E." CA: California Department of Conservation, Division of Oil, Gas, and Geothermal Resources. Retrieved December, 2012 (http://owr.conservation.ca.gov/Well/WellDetailPage.aspx?domsapp=1&apinum=0192059)

California Department of Conservation, Division of Oil, Gas, and Geothermal Resources 2013. "Well Data, N.E.C.K. Petroleum Company, Well: Mohawk-Bloss 1, Section: 6, Township: 8S, Range: 16E." CA: California Department of Conservation, Division of Oil, Gas, and Geothermal Resources. Retrieved June, 2013 (http://owr.conservation.ca.gov/Well/WellDetailPage.aspx?domsapp=1&apinum=04720004)

Cara, Fabrizio, Giovanna Cultrera, Riccardo Mario Azzara, Valerio De Rubeis, Giuseppe Di Giulio, Maria Stella Giammarinaro, Patrizia Tosi, Paola Vallone, and Antonio Rovelli. 2008. "Microtremor Measurements in the City of Palermo, Italy: Analysis of the Correlation between Local Geology and Damage." *Bulletin of the Seismological Society of America* 98(3):1354-72.

Delgado, J., C. López Casado, J. Giner, A. Estévez, A. Cuenca, and S. Molina. 2000. "Microtremors as a Geophysical Exploration Tool: Applications and Limitations." *Pure and Applied Geophysics* 157(2000):1445-62.

Haplosciences 2000-2007. "Sound-Behavior of Waves." Haplosciences. Retrieved July, 2013 (http://onlinephys.com/waves2/15_19.jpg).

Holbrook, Steven W. and Walter D. Mooney. 1987. "The crustal structure of the axis of the Great Valley, California, from seismic refraction measurements." *Tectonophysics* 140(1987):49-63.

Incorporated Research Institutions for Seismology 2012. "Timseries Webservice URL Builder." Washington, DC: Incorporated Research Institutions for Seismology. Retrieved April 12, 2012 (http://www.iris.edu/ws/builder/timeseries/).

Incorporated Research Institutions for Seismology 2012. "Network map for USArray Transportable Array (NSF EarthScope Project)." Washington, DC: Incorporated Research Institutions for Seismology. Retrieved April 12, 2012 (http://www.iris.edu/gmap/TA).

Ingersoll, Raymond V. 1988. "Tectonics of sedimentary basins." *Geological Society of America Bulletin* 100:1704-19.

Lane, John W., Jr., Eric A. White, Gregory V. Steele, and James C. Cannia. 2008. "Estimation of Bedrock Depth Using the Horizontal-to-Vertical (H/V) Ambient-Noise Seismic Method." *Symposium on the Application of Geophysics to Engineering and Environmental Problems* 1-13.

Lermo, Javier and Francisco J. Chávez-García. 1993. "Site Effect Evaluation Using Spectral Ratios with Only One Station." *Bulletin of the Seismological Society of America* 83(5):1574-94.

Pujol, T. J. 1954. "Structure Section A-A', Township: 1-5S Range: 6-10E Modesto Area." *Tidewater Oil Company*.

Pujol, T. J. 1958. "Contours on Top Basement, Township: 1-5S Range: 6-10E Modesto Area." *Tidewater Oil Company*.

Seht, Malte Ibs-von and Jürgen Wholenberg. 1999. "Microtremor Measurements Used to Map Thickness of Soft Sediments." *Bulletin of the Seismological Society of America* 89(1):250-59.

Yilmaz, A. 2001. "Seismic Data Analysis" *Society of Exploration Geophysics*.

Yuncha, Zakaria Al and Francisco Luzón. 2000. "On the Horizontal-to-Vertical Spectral Ratio in Sedimentary Basins." *Bulletin of the Seismological Society of America* 90(4):1101-06.

APPENDIX

Appendix A. Cross-Section Modesto Area by Pujol, 1954.

Appendix B. Top Basement Map Modesto Area by Pujol, 1958.

Appendix C. Sonic Log: Redfern Ranches Well #A-1, Phillips Petroleum Company.

Appendix D. Matlab Code: ExampleRefCodes.m used to analyze seismic data and calculate resonant frequencies.

Appendix E. rsac.m

Appendix F. centeredFFT.m

Appendix G. lpfilter.m

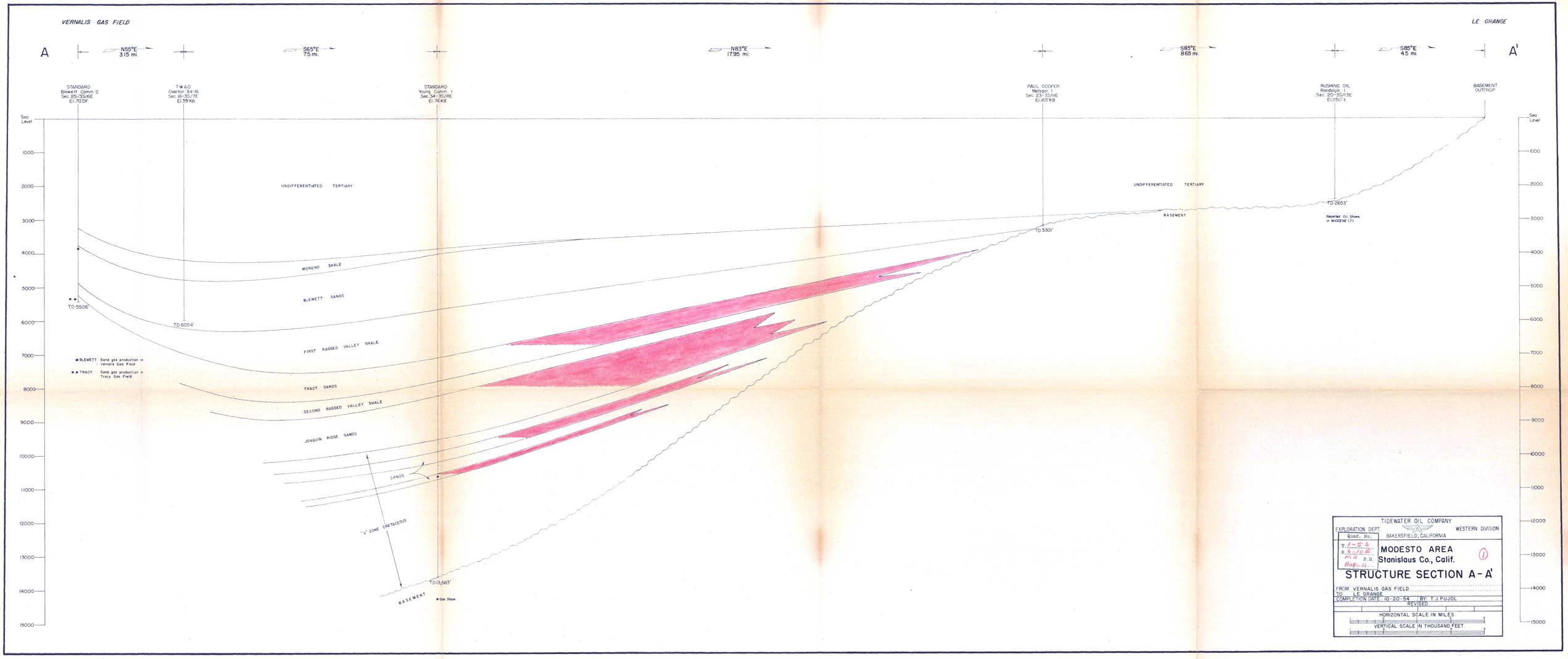
VERNALIS GAS FIELD
LE GRANGE
A
A'
N55°E 3.15 mi.
S65°E 7.5 mi.
N83°E 17.95 mi.
S85°E 8.65 mi.
S85°E 4.5 mi.
STANDARD Blewett Comm. 2 Sec. 25-3S/6E El. 70' DF
T.W.A.O. Overton 34-16 Sec. 16-3S/7E El. 39' KB
STANDARD Young Comm. 1 Sec. 34-3S/8E El. 74' KB
PAUL COOPER Mariger 1 Sec. 23-3S/11E El. 165' KB
RUSHING OIL Randolph 1 Sec. 20-3S/13E El. 250' ±
BASEMENT OUTCROP
Sea Level
1000
2000
3000
4000
5000
6000
7000
8000
9000
10000
11000
12000
13000
14000
15000
UNDIFFERENTIATED TERTIARY
UNDIFFERENTIATED TERTIARY
MORENO SHALE
BLEWETT SANDS
FIRST RAGGED VALLEY SHALE
TRACY SANDS
SECOND RAGGED VALLEY SHALE
JOAQUIN RIDGE SANDS
SANDS
"G" ZONE CRETACEOUS
BASEMENT
BASEMENT
T.D. 5506'
T.D. 6054'
T.D. 3301'
T.D. 2653'
Reported Oil Shows in MIOCENE (?)
T.D. 13,683'
* Gas Show
* BLEWETT Sand gas production in Vernalis Gas Field
* * TRACY Sand gas production in Tracy Gas Field
TIDEWATER OIL COMPANY
EXPLORATION DEPT.
WESTERN DIVISION
Quad. No.
BAKERSFIELD, CALIFORNIA
T. 1-S S
R. 6-10 E.
M.D. B.M.
Map No. 11
MODESTO AREA
Stanislaus Co., Calif.
1
STRUCTURE SECTION A-A'
FROM VERNALIS GAS FIELD
TO LE GRANGE
COMPLETION DATE 10-20-54
BY: T.J. PUJOL
REVISED
HORIZONTAL SCALE IN MILES
VERTICAL SCALE IN THOUSAND FEET

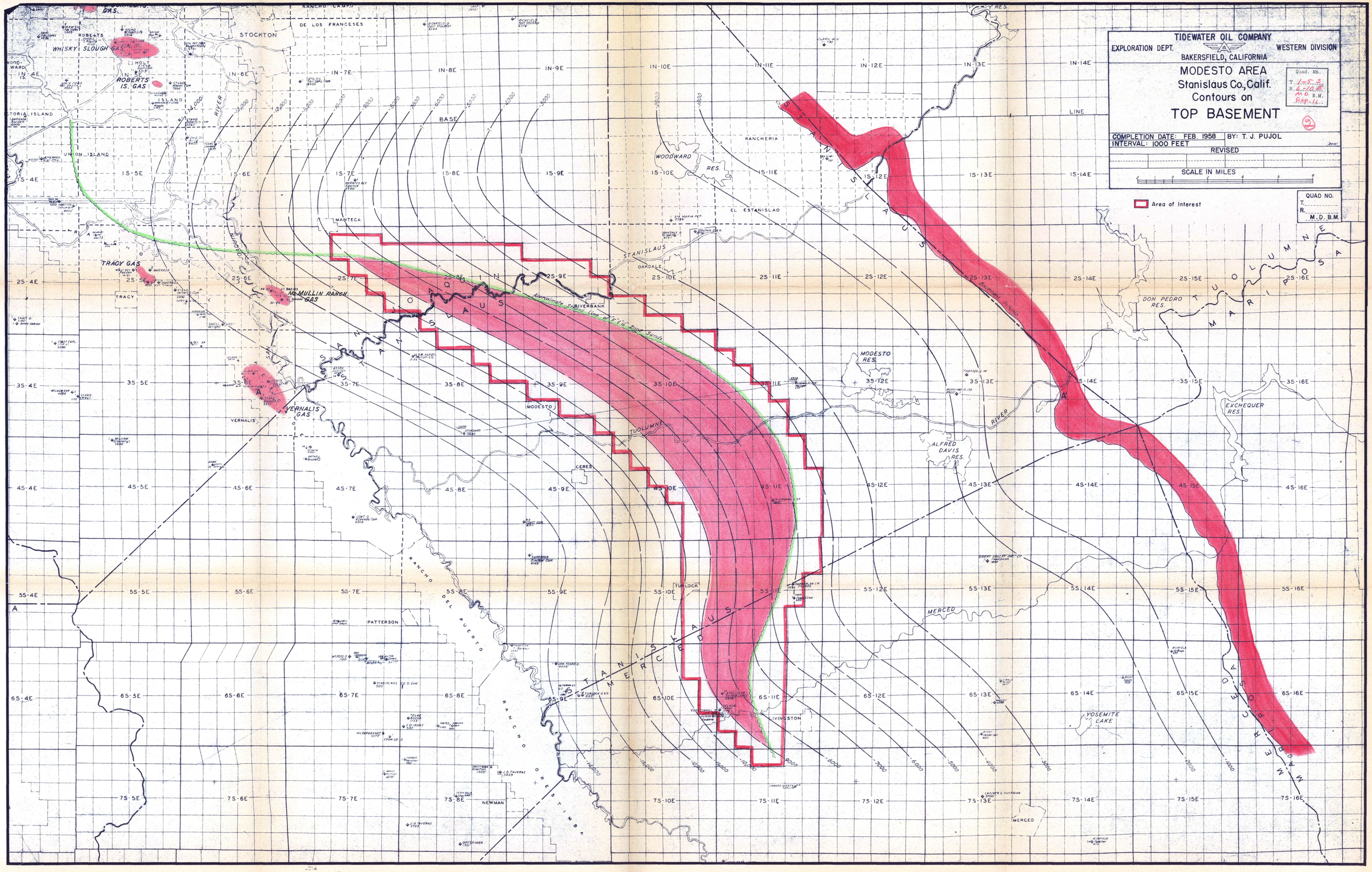
TIDEWATER OIL COMPANY
EXPLORATION DEPT.
WESTERN DIVISION
BAKERSFIELD, CALIFORNIA
MODESTO AREA
Stanislaus Co., Calif.
Contours on
TOP BASEMENT
Quad. No.
T. 1-5-3
R. 6-10-E
M.D.B.M.
Rep. 11
COMPLETION DATE: FEB. 1958
BY: T. J. PUJOL
INTERVAL: 1000 FEET
REVISED
SCALE IN MILES
Area of Interest
QUAD NO.
T.
R.
M.D.B.M.
Approximate Southerly Line of "Eocene" Tone Sands
Basement Outcrop
STOCKTON
DE LOS FRANCESES
WHISKY SLOUGH GAS
ROBERTS IS. GAS
ROBERTS
WOODWARD IS.
VICTORIA ISLAND
UNION ISLAND
RIVER
BASE
LINE
RANCHERIA
WOODWARD RES.
EL ESTANISLAO
MANTECA
TRACY GAS
TRACY
McMULLIN RANCH GAS
STANISLAUS
OAKDALE
RIVERBANK
VERNALIS GAS
VERNALIS
MODESTO
TUOLUMNE
CERES
MODESTO RES.
ALFRED DAVIS RES.
DON PEDRO RES.
EXCHEQUER RES.
TURLOCK
PATTERSON
RANCHO DEL PUERTO
RANCHO ORESTIMBA
NEWMAN
IVINGSTON
MERCED
YOSEMITE LAKE
SAN JOAQUIN
STANISLAUS
TUOLUMNE
MARIPOSA
MERCED
A
A'

APPENDIX D

ExampleRefCodes.m

```
%% Calculate The H/V Transfer Funciton from Microtremor Data

%% Load Seismic Data Code (Vertical Channel)
% Let d1 equal our matrix with vertical channel data from the seismometer
% T05C in the TA seismic array

d1 = rsac('T05C.BHZ.2005.VEL.SAC');

%% Plot Code for Data

figure(1); plot(d1(:,1),d1(:,2)); grid on ; xlabel('Seconds');...
    ylabel('Ground Velocity (m/s)');

%% Run centeredFFT (Frequency Spectrum) for Vertical Channel
% Remove Mean and Taper Endpoints

zdata = d1(:,2); zdata = detrend(zdata,'constant');
zdata = zdata.*tukeywin(length(zdata),0.1);

% Run centeredFFT

[X1 freq] = centeredFFT(zdata,(1/d1(1,3)));

% Plot Freq Spectrum

figure(2); plot(freq,abs(X1)); xlabel('Frequency (Hz)');...
    ylabel('Spectral Amplitude'); grid on;

%% LP Filter Code

lpfData = lpfilter(zdata,0.5,(1/d1(1,3)),-1);
figure(77); plot(d1(:,1),lpfData);grid on; xlabel('Seconds');...
    ylabel ('Ground Velocity (m/s)');

%% LP Filter Data FFT

[X1 freq] = centeredFFT(lpfData,(1/d1(1,3)));
figure(3); plot(freq,abs(X1)); xlabel('Frequency (Hz)');...
    ylabel('Spectral Amplitude');grid on;

% 'Water Level' Filter

X1=X1+0.000000001;

%% Load Seismic Data Code (North-South Channel)
% Let d2 equal our matrix with north-south channel data from the
% seismometer T05C in the TA seismic array
```

```
d2 = rsac('T05C.BHN.2005.VEL.SAC');

%% Plot Code for Data
figure(1); plot(d2(:,1),d2(:,2)); grid on; xlabel('seconds');...
    ylabel('Ground Velocity (m/s)');

%% Run centeredFFT (Frequency Spectrum) for N-S Channel
% Remove Mean and Taper Endpoints

ndata = d2(:,2); ndata = detrend(ndata,'constant');
ndata = ndata.*tukeywin(length(ndata),0.1);

% Run centeredFFT

[X2 freq] = centeredFFT(ndata,(1/d2(1,3)));

% Plot Freq Spectrum

figure(2); plot(freq,abs(X2)); xlabel('Frequency (Hz)');...
    ylabel('Spectral Amplitude'); grid on;

%% LP Filter Code

lpfData = lpfilter(ndata,0.5,(1/d2(1,3)),-1);
figure(77); plot(d2(:,1),lpfData); grid on;

%% LPF Data FFT

[X2 freq] = centeredFFT(lpfData,(1/d2(1,3)));
figure(3); plot(freq,abs(X2)); xlabel('Frequency (Hz)');...
    ylabel('Spectral Amplitude'); grid on;

%% Load Seismic Data Code (East-West Channel)
% Let d3 equal our matrix with east-west channel data from the seismometer
% T05C in the TA seismic array

d3 = rsac('T05C.BHE.2005.VEL.SAC');

%% Plot Code for Data

figure(1); plot(d3(:,1),d3(:,2)); grid on; xlabel('Seconds');...
    ylabel('Ground Velocity (m/s)');

%% Run centeredFFT (Frequency Spectrum) for E-W data
% Remove Mean and Taper Endpoints

edata = d3(:,2); edata = detrend(edata,'constant');
edata = edata.*tukeywin(length(edata),0.1);

% Run centeredFFT

[X3 freq] = centeredFFT(edata,(1/d3(1,3)));
```

```
% Plot Freq Spectrum

figure(2); plot(freq,abs(X3)); xlabel('Frequency (Hz)');...
    ylabel('Spectral Amplitude'); grid on;

%% LP Filter Code

lpfData = lpfilter(edata,0.5,(1/d3(1,3)),-1);
figure(77); plot(d3(:,1),lpfData); grid on;

%% LPF Data FFT

[X3 freq] = centeredFFT(lpfData,(1/d3(1,3)));
figure(3); plot(freq,abs(X3)); xlabel('Frequency (Hz)');...
    ylabel('Spectral Amplitude');grid on;

%% Transfer Function Calculation for H/V ratio

t=sqrt((X2.^2 + X3.^2)./(2.*X1.^2));
t=abs(t);
figure(4445); plot(freq,t); xlabel('Frequency (Hz)');...
    ylabel('Spectral Amplitude');grid on
```

APPENDIX E

```
%RSAC    Read SAC binary files.
%    RSAC('sacfile') reads in a SAC (seismic analysis code) binary
%    format file into a 3-column vector.
%    Column 1 contains time values.
%    Column 2 contains amplitude values.
%    Column 3 contains all SAC header information.
%    Default byte order is big-endian.  M-file can be set to default
%    little-endian byte order.
%
%    usage:  output = rsac('sacfile')
%
%    Examples:
%
%    KATH = rsac('KATH.R');
%    plot(KATH(:,1),KATH(:,2))
%
%    [SQRL, AAK] = rsac('SQRL.R','AAK.R');
%
%    by Michael Thorne (4/2004)   mthorne@asu.edu

function [varargout] = rsac(varargin);

for nrecs = 1:nargin

  sacfile = varargin{nrecs};

%-----------------------------------------------------------------------------
%    Default byte-order
%    endian  = 'big-endian' byte order (e.g., UNIX)
%            = 'little-endian' byte order (e.g., LINUX)

endian = 'little-endian';

if strcmp(endian,'big-endian')
  fid = fopen(sacfile,'r','ieee-be');
elseif strcmp(endian,'little-endian')
  fid = fopen(sacfile,'r','ieee-le');
end

% read in single precision real header variables:
%-----------------------------------------------------------------------------
for i=1:70
  h(i) = fread(fid,1,'single');
end

% read in single precision integer header variables:
%-----------------------------------------------------------------------------
for i=71:105
  h(i) = fread(fid,1,'int32');
end
```

```
% Check header version = 6 and issue warning
%-------------------------------------------------------------------------
% If the header version is not NVHDR == 6 then the sacfile is likely of the
% opposite byte order.  This will give h(77) some ridiculously large
% number.  NVHDR can also be 4 or 5.  In this case it is an old SAC file
% and rsac cannot read this file in.  To correct, read the SAC file into
% the newest verson of SAC and w over.
%
if (h(77) == 4 | h(77) == 5)
    message = strcat('NVHDR = 4 or 5. File: "',sacfile,'" may be from an old
version of SAC.');
    error(message)
elseif h(77) ~= 6
    message = strcat('Current rsac byte order: "',endian,'". File:
"',sacfile,'" may be of opposite byte-order.');
    error(message)
end

% read in logical header variables
%-------------------------------------------------------------------------
for i=106:110
  h(i) = fread(fid,1,'int32');
end

% read in character header variables
%-------------------------------------------------------------------------
for i=111:302
  h(i) = (fread(fid,1,'char'))';
end

% read in amplitudes
%-------------------------------------------------------------------------

YARRAY     = fread(fid,'single');

if h(106) == 1
  XARRAY = (linspace(h(6),h(7),h(80)))';
else
  error('LEVEN must = 1; SAC file not evenly spaced')
end

% add header signature for testing files for SAC format
%-------------------------------------------------------------------------
h(303) = 77;
h(304) = 73;
h(305) = 75;
h(306) = 69;

% arrange output files
%-------------------------------------------------------------------------
OUTPUT(:,1) = XARRAY;
OUTPUT(:,2) = YARRAY;
OUTPUT(1:306,3) = h(1:306)';

%pad xarray and yarray with NaN if smaller than header field
```

```
if h(80) < 306
  OUTPUT((h(80)+1):306,1) = NaN;
  OUTPUT((h(80)+1):306,2) = NaN;
end

fclose(fid);

varargout{nrecs} = OUTPUT;

end
```

APPENDIX F

```
function [X,freq]=centeredFFT(x,Fs)
%this is a custom function that helps in plotting the two-sided spectrum
%x is the signal that is to be transformed
%Fs is the sampling rate

N = length(x);

%this part of the code generates that frequency axis
if mod(N,2) == 0
    k = -N/2:N/2-1; % N even
else
    k = -(N-1)/2:(N-1)/2; % N odd
end
T = N/Fs;
freq = k/T;  %the frequency axis

%takes the fft of the signal, and adjusts the amplitude accordingly
X = fft(x)/N; %/N normalize the data
X = fftshift(X); %shifts the fft data so that it is centered
```

APPENDIX G

```
function[lpfData] = lpfilter(data,lpcorner,samplingFrequency,order)
%
% Butterworth low pass filter
%
% INPUTS:
% data: 1-d vector of data points
% lpcorner: frequencies above are cut, or...frequencies below are preserved
% samplingFrequency: frequency of data sampling, Hz
% order: filter order. Defaults to 4 if not specified, or input as -1
%
% EXAMPLE USAGE:
% [lpfData] = lpfilter(data,2,40,10)
% [lpfData] = lpfilter(data,0.5,200,-1)
%


%% Check Inputs...need to fix this up....

if nargin > 4 || nargin < 1
    fprintf('incorrect number of inputs\n')
    fprintf('type: help lpfilter\n')
    return
elseif nargin < 2
    fprintf('must choose a corner frequency!\n')
    fprintf('type: help lpfilter\n')
    return
elseif nargin < 3
    fprintf('must input a sampling frequency\n')
    fprintf('type: help lpfilter\n')
elseif nargin == 3
    fprintf('defaulting to 4th order\n')
    order = 4;
end

if nargin == 4 && order == -1
    order = 4;
end



%%  Low Pass Filter Constructed & Applied Here

fNorm = lpcorner / (samplingFrequency/2);
[b a] = butter(order,fNorm,'low');
lpfData = filtfilt(b,a,data);
```